Electronic Supplementary Material (ESI) for Nanoscale.

Supporting Information

Susana Ramos-Terrón,[†,] David Alba-Molina,[†,‡,*] Maria de los Ángeles Varo-Santos,[†] Manuel Cano,[†] Juan José Giner-Casares[†] and Gustavo de Miguel[†]*

[†] Departamento de Química Física y Termodinámica Aplicada, Instituto Universitario de Investigación en Química Fina y Nanoquímica, IUNAN, Universidad de Córdoba, Campus de Rabanales, Edificio Marie Curie, E-14071 Córdoba, Spain

[‡] Currently at the Maimónides Institute of Biomedical Research (IMIBIC), Reina Sofía University Hospital, Córdoba, Spain

* These authors contributed equally to this work

Corresponding Author

E-mail: jjginer@uco.es and gmiguel@uco.es

Table of Contents

Section 1. Materials Synthesis

- **Starting Materials**

All starting materials for synthesis were commercially purchased and used as received. Tetrachloroauric (III) Acid ($HAuCl_4$, >99.9%), Sodium Citrate (>99.0%), Polyvinylpyrrolidone (PVP, average mol wt 10,000), Tetraetoxisilane (TEOS, 98.0%) and Ammonia (28-30%) were purchased from Sigma-Aldrich. Methylammonium iodide (MAI, 98%) and Phenethylammonium iodide (PEAI, 98%) were supplied from Greatcell Solar. Lead iodide (PbI_2, 99%) was purchased from Tokyo Chemical Industry (TCI). *N*,*N*-Dimethylformamide (DMF) 99.8% extra dry over molecular sieve, AcroSeal; Dimethyl sulfoxide (DMSO) 99.7% extra dry over molecular sieve, AcroSeal; and Chlorobenzene extra dry over molecular sieve, AcroSeal were purchased from Acros Organics.

The amorphous glass were purchased from Pilkington. Isopropyl alcohol (technical grade, 99.5%) and the soap (decon90) were purchased from PanReac AppliChem and Decon, respectively.

- **Synthesis of $Au@SiO_2$ NPs**

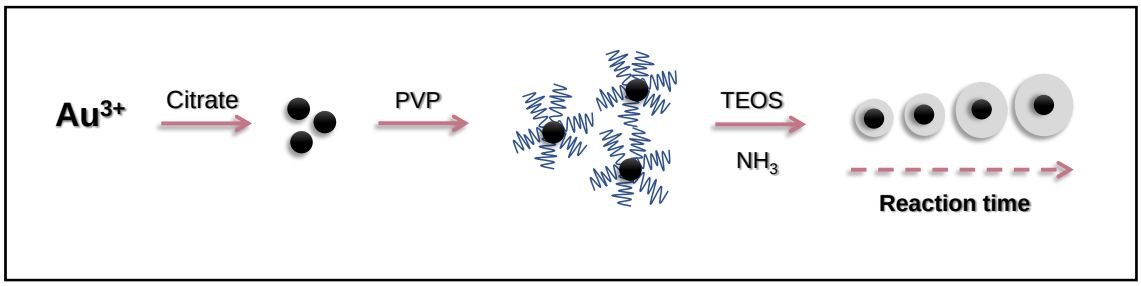

Scheme S1. Reaction outline of the synthesis $Au@SiO_2$ NPs through the different steps.

- Synthesis of citrate-stabilized gold nanoparticles (AuNPs@Citrate)

20 nm citrate capped AuNPs with a uniform quasi-spherical shape and a narrow size distribution were synthesized according to a kinetically controlled seeded growth strategy via reduction of $HAuCl_4$ mediated by sodium citrate.[1] Briefly, 250 mL of 2.2 mM sodium citrate solution was heated in a 500 mL three-necked round flask for 20 minutes under vigorous stirring. Upon reaching 96 ºC, 1 mL of 42 mM $HAuCl_4$ was injected. After 20 minutes the temperature was decreased until 90ºC, once the temperature was stable, another 1 mL of 42 mM $HAuCl_4$ was injected to obtain citrate-stabilized AuNPs with a diameter of ca. 20 nm.

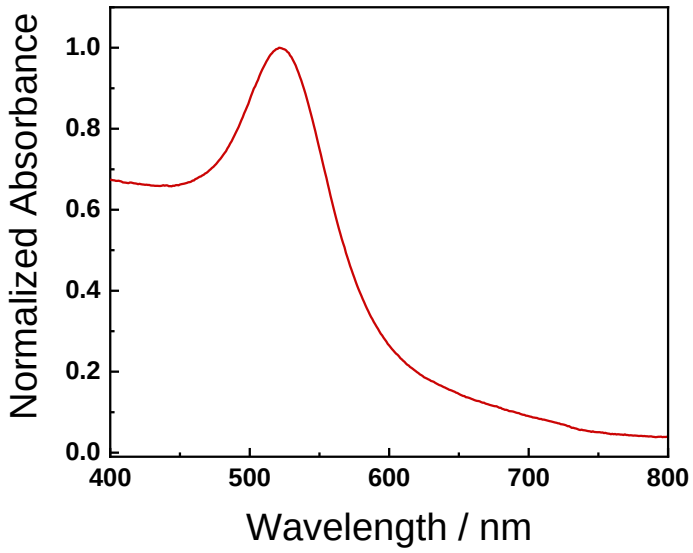

Figure S1. Absorption spectrum of gold nanoparticles stabilized in citrate (AuNP@Citrate) after two growth steps.

- Ligand-exchange process (AuNPs@PVP)

Prior to silica coating of AuNPs, a ligand exchange process was carried out to obtain Polyvinylpyrrolidone (PVP) capped AuNPs based on a simple concentration gradient.[2] PVP capping ligand provides higher affinity to silica particles, facilitating the silica shell formation and, growth[3,4] also allows dispersion in certain organic solvents. For this, 250 mL of the previously synthesized citrate-stabilized AuNPs were centrifuged at 7500 rpm for 30 minutes. Next, the supernatant was discarded, and the pellet was suspended into 125 mL of ultrapure water. Subsequently, 0.96 mL of an aqueous solution containing 24.87 mg of PVP was added to the latter colloidal dispersion, and the whole mixture was stirred for 24 hours before the silica coating process.

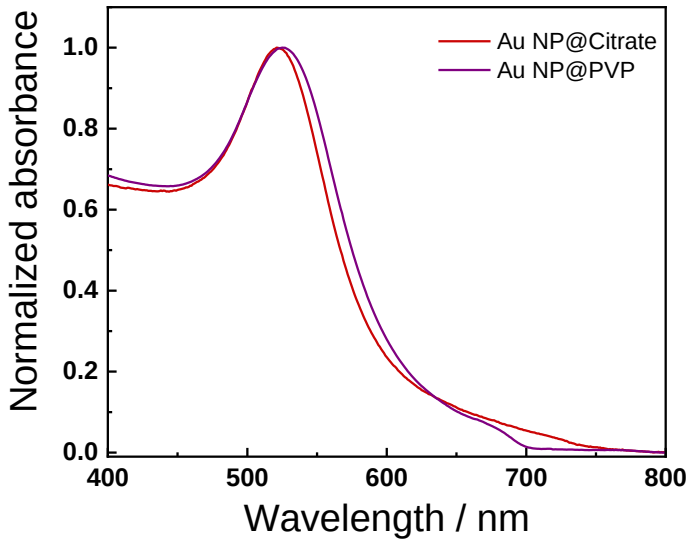

Figure S2. Absorption spectra of gold nanoparticles stabilized in citrate (red) and PVP (purple) after ligand exchange.

- Silica coating process (core-shell Au@SiO_2 NPs)

Core-shell Au@SiO_2 NPs were prepared with different thickness of silica shell using tetraethyl orthosilicate (TEOS) mediated synthesis based on Stöber like method.[4,5] 15 mL of PVP capped Au NPs obtained above were centrifuged at 7500 rpm for 30 minutes. The pellet containing AuNPs@PVP was suspended into 1.5 mL of ultrapure water, and subsequently 13.5 mL of isopropanol was added under vigorous stirring. To the latter mixture, 0.282 mL of concentrated ammonia (~28%) and 7.45 μL of TEOS (98%) were added. After 10 minutes of mixing at room temperature, the reaction mixture was kept into a fridge (4 ºC) to slow down the silica shell growth. Incubation time of the latter mixture was used as parameter to regulate the silica shell growth (Figure S3). Our experimental conditions allow the use of longer incubation times to minimize the formation of silica islands.[4] To stop the reaction at the different time courses, the core-shell Au@SiO_2 NPs were purified by centrifugation (7500 rpm for 30 min) and washed twice with water. Finally, the purified core-shell Au@SiO_2 NPs were suspended into 5 mL of pure DMF (final volume) and stored until use.

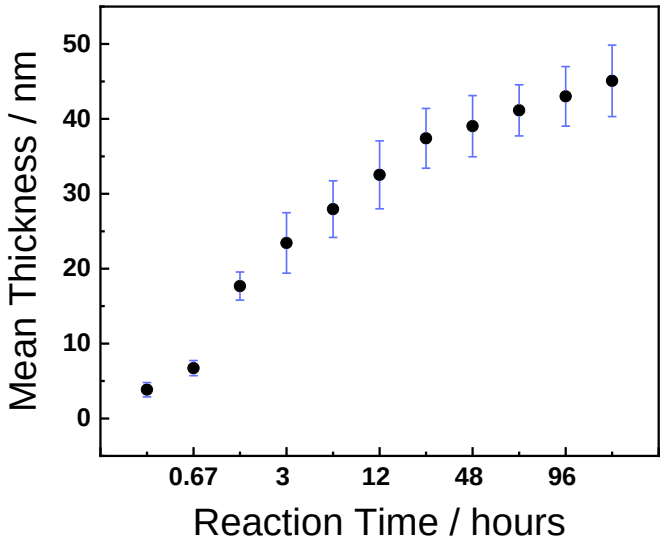

Figure S3. Mean thickness of silica shell as a function of the reaction time.

- **Perovskite Precursor Solutions**

For the $MAPbI_3$ perovskite, a stoichiometric precursor solution was prepared by mixing MAI and PbI_2 in DMF/DMSO. The solution was adjusted to the relative humidity of the environment (40% R.H.) by the Pb/DMSO ratio.[6]

In all prepared solutions the PbI_2 molarity was equal to 0.3.

Section 2. Film Fabrication

- **Substrate Preparation**

All substrates (amorphous glass 2x2 cm^2) were cleaned by a sequential sonication treatment in Decon 90 solution, Milli-Q water and isopropyl alcohol. Thereupon, they were dried by using compressed air. The substrates were treated with ultraviolet ozone for 15 min before the deposition.

- **Au@SiO_2 NPs Deposition**

The Au@SiO_2 NPs were deposited onto the amorphous glass substrate by spray pyrolysis using 0.5 mL of Au@SiO_2 NPs (with Au concentration of 0.7 mM) suspended in DMF. The resulting films were annealed at 100 °C on a hot plate to remove solvent traces. The experimental conditions were optimized for depositing a similar amount of Au NP in all cases. Note that small variations might be found due to the larger size of the Au NP coated with thick silica layer.

- **Perovskite Deposition**

The $MAPbI_3$ perovskite films have been deposited by spin coating using a process previously reported.[6] The perovskite precursor solution (50 µL) was deposited on the substrates at 4000 rpm for 50 s. During this step, just before the white solid begins to crystallize in the substrate, 200 µL of chlorobenzene was poured onto the films. Then, the films were annealed at 100 ºC on a hot plate for 3 min.

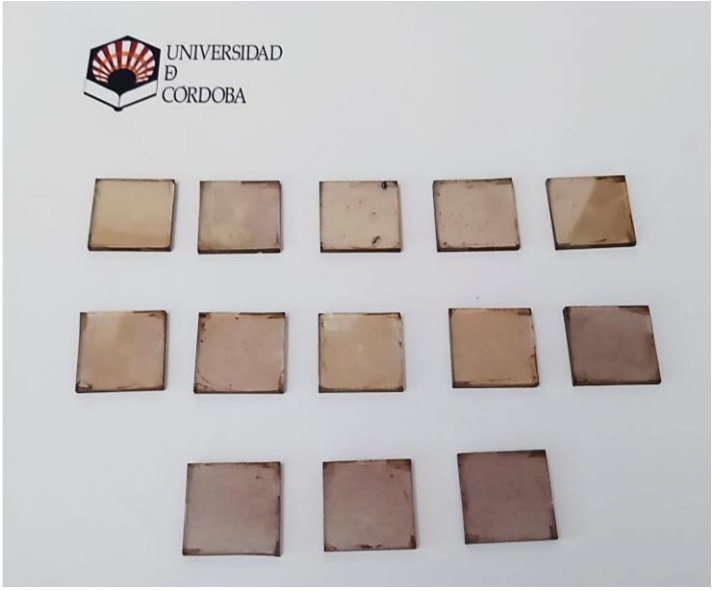

Figure S4. Photographs of the layers of the Au@SiO_2 NP/$MAPbI_3$ composite. From left to right and up to down, an increasing thickness of the SiO_2 shell is employed.

Section 3. Materials and film characterization

- **UV-Vis Absorption Spectroscopy**

The measurements were performed at room temperature (~25 °C) using a UV−Vis spectrometer CARY 100. The range of the measurement was from 400 to 800 nm with 1 nm step in all cases.

- **X-Ray Diffraction (XRD) Measurements**

X-ray diffraction experiments for all of the samples were performed using a Bruker D8 DISCOVER diffractometer operating at 40 kV and 40 mA and using Cu Kα radiation (1.54060 Å). The measurements were done from 2 to 40° Bragg angles.

- **Transmission Electron Microscope (TEM)**

TEM images were recorded in a JOEL JEM 1400 instrument (Tokyo, Japan), assembled with a charge-coupled camera device, at an accelerating voltage of 80 kV. Samples for TEM were prepared by drying a diluted dispersion of the particles in ambient conditions on 200 mesh copper grids coated with

Formvar/carbon films. The size of the AuNPs was quantified by ImageJ software (National Institute of Health (NIH), USA).

- **Scanning Electron Microscopy (SEM)**

SEM images were recorded in a JOEL JSM 7800F microscope working at 2 kV. The work distances were ≈ 10 mm for all cases and 22000x magnification. Energy-dispersive X-ray (EDX) was performed using a silicon drift detector (Oxford Instruments).

- **Steady-State and Time-Resolved PL Measurements**

Steady state photoluminescence spectra were recorded with an FLS980 (Edinburgh Instruments) fluorescence spectrometer using a 450 W Xe1 xenon arc lamp and an R298P photomultiplier as the detector. Time-resolved fluorescence measurements were accomplished through the time-correlated single photon counting (TCSPC) technique, using the same FLS980 (Edinburgh Instruments) photoluminescence spectrometer. The samples were excited at 406.4 nm with an 86.8 ps pulse width diode laser using an R2658P photomultiplier as the detector.

- **PL Quantum Yield Measurement (PLQY)**

The PLQYs were measured using an integrating sphere coupled to an FLS980 photoluminescence spectrometer. The FLS980 was equipped with double monochromators, a 450 W Xenon lamp and a PMT-R2658P detector. A neutral density filter (OD = 3) was placed in the emission path in order to measure excitation region of the spectrum without detector saturation effects.

Section 4. Calculated and experimental XRD

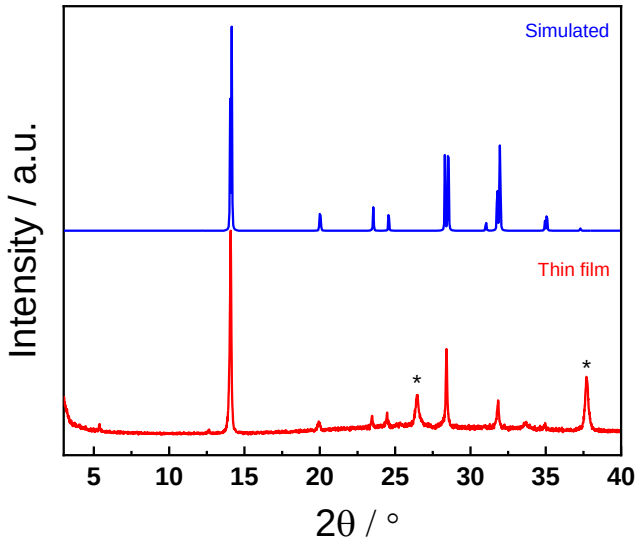

Figure S5. Experimental thin film (red line) and simulated (blue line) X-ray diffraction (XRD) patterns of the of $MAPbI_3$ perovskite. Asterisk indicates an FTO signal.

Section 5. Additional UV-Vis and PL data

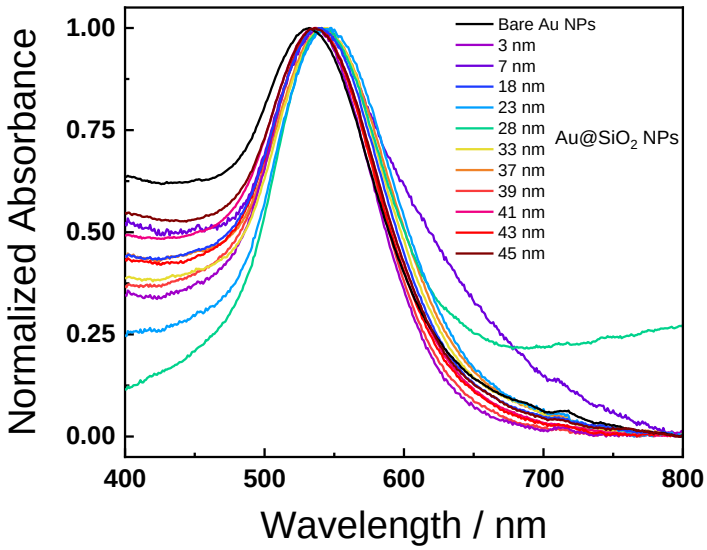

Figure S6. UV-Visible absorption spectra of the Au@SiO_2 NPs in DMF with different SiO_2 thickness.

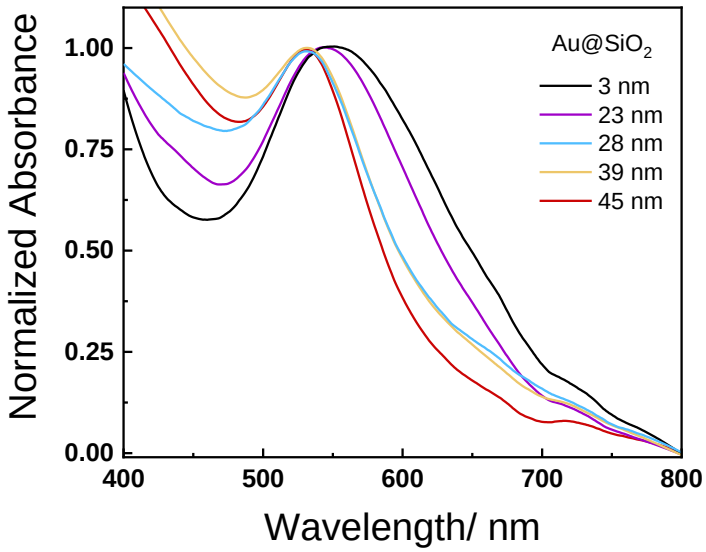

Figure S7. UV-Visible absorption spectra of the Au@SiO_2 NPs layers deposited by spray pyrolysis with different SiO_2 thickness.

Section 6. Additional SEM data

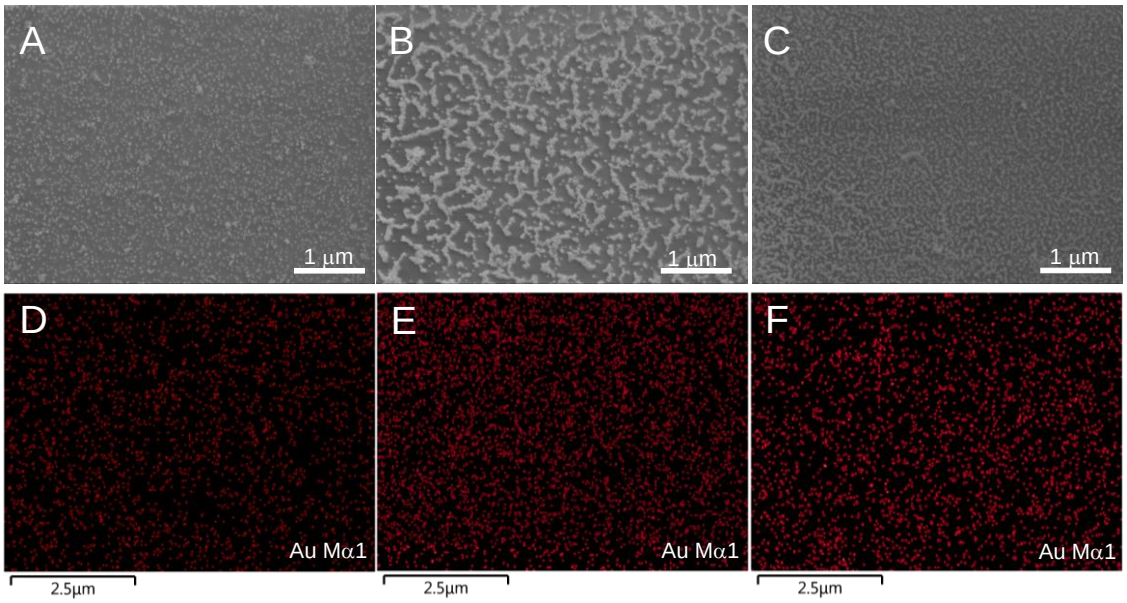

Figure S8. SEM images (upper panel) and gold elemental mapping (lower panel) of the thin layers of Au NPs deposited with spray pyrolysis from three different Au concentrations: 0.14 mM (A, D), 0.42 mM (B, E) and 0.70 mM (C, F).

Table S1. PL average time constants (τ_{PL}) and PL quantum yield (Φ_{PL}) of $MAPbI_3$ perovskite films deposited on top of a layer of Au@SiO_2 NPs with different SiO_2 thickness obtained from a triexponential fit of the data. λ_{exc} = 400 nm.

			SiO_2 thickness / nm						
	No Au NPs	**Bare Au NPs**	**6.7**	**17.7**	**28**	**37**	**39**	**41**	**45**
τ_{PL} / ns	251	1.0	4.2	15.1	29.2	56.7	88.0	173.2	230.1
Φ_{PL}	0.03	0.0003	0.0027	0.0036	0.012	0.019	0.025	0.028	0.029

Bibliography

(1) Alba-Molina, D.; Puente Santiago, A. R.; Giner-Casares, J. J.; Martín-Romero, M. T.; Camacho, L.; Luque, R.; Cano, M. Citrate-Stabilized Gold Nanoparticles as High-Performance Electrocatalysts: The Role of Size in the Electroreduction of Oxygen. *J. Phys. Chem. C* **2019**, *123* (15), 9807–9812. https://doi.org/10.1021/acs.jpcc.9b00249.

(2) Alba-Molina, D.; Puente Santiago, A. R.; Giner-Casares, J. J.; Rodríguez-Castellón, E.; Martín-Romero, M. T.; Camacho, L.; Luque, R.; Cano, M. Tailoring the ORR and HER Electrocatalytic Performances of Gold Nanoparticles through Metal-Ligand Interfaces. *J. Mater. Chem. A* **2019**, *7* (35), 20425–20434. https://doi.org/10.1039/c9ta05492h.

(3) Robinson, S.; Williams, P. A. Inhibition of Protein Adsorption onto Silica by Polyvinylpyrrolidone. *Langmuir* **2002**, *18* (23), 8743–8748. https://doi.org/10.1021/la020376l.

(4) Vanderkooy, A.; Chen, Y.; Gonzaga, F.; Brook, M. A. Silica Shell/Gold Core Nanoparticles: Correlating Shell Thickness with the Plasmonic Red Shift upon Aggregation. *ACS Appl. Mater. Interfaces* **2011**, *3* (10), 3942–3947. https://doi.org/10.1021/am200825f.

(5) Liz-marzán, L. M.; Giersig, M.; Mulvaney, P. Synthesis of Nanosized Gold - Silica Core - Shell Particles. **1996**, *7463* (5), 4329–4335.

(6) Contreras-Bernal, L.; Aranda, C.; Valles-Pelarda, M.; Ngo, T. T.; Ramos-Terrón, S.; Gallardo, J. J.; Navas, J.; Guerrero, A.; Mora-Seró, I.; Idígoras, J.; et al. Homeopathic Perovskite Solar Cells: Effect of Humidity during Fabrication on the Performance and Stability of the Device. *J. Phys. Chem. C* **2018**, *122* (10), 5341–5348. https://doi.org/10.1021/acs.jpcc.8b01558.

(7) Ramos-Terrón, S.; Jodlowski, A. D.; Verdugo-Escamilla, C.; Camacho, L.; De Miguel, G. Relaxing the Goldschmidt Tolerance Factor: Sizable Incorporation of the Guanidinium Cation into a Two-Dimensional Ruddlesden-Popper Perovskite. *Chem. Mater.* **2020**, *32* (9), 4024–4037. https://doi.org/10.1021/acs.chemmater.0c00613.

(8) Ramos-Terrón, S.; Verdugo-Escamilla, C.; Camacho, L.; De Miguel, G. A-Site Cation Engineering in 2D Ruddlesden–Popper $(BA)_2(MA_{1-X}Ax)_2Pb_3I_{10}$ Perovskite Films. Adv. Opt. Mater. **2021**, 2100114, https://doi.org/10.1002/adom.202100114.